Research in Astron. Astrophys. **2012** Vol. **12** No. **3**, 345–358
http://www.raa-journal.org *http://www.iop.org/journals/raa*

***R**esearch in*
***A**stronomy and*
***A**strophysics*

Calculation of the structural properties of asymmetrical nuclear matter

Gholam Hossein Bordbar[1,2] and Hamideh Nadgaran[1]

[1] Department of Physics, Shiraz University, Shiraz 71454, Iran; *bordbar@physics.susc.ac.ir*
[2] Research Institute for Astronomy and Astrophysics of Maragha, P.O. Box 55134-441, Maragha 55177-36698, Iran

Received 2011 May 9; accepted 2011 November 1

Abstract The structural properties of asymmetrical nuclear matter have been calculated, employing the AV_{18} potential for different values of proton to neutron ratio. These calculations have also been made for the case of symmetrical nuclear matter with the UV_{14}, AV_{14} and AV_{18} potentials. In our calculations, we used the lowest order constrained variational method to compute the correlation function of the system.

Key words: stars: neutron — dense matter — equation of state

1 INTRODUCTION

The interpretation of many astrophysical phenomena depends on a profound understanding of different areas of physics. Nuclear physics plays an important role in determining the energy and evolution of stellar matter. Most of the calculations for asymmetrical nuclear matter have a close relationship with astrophysics. These studies are also potentially useful for understanding the effective nucleon–nucleon interactions in dense asymmetrical nuclear matter, an important ingredient in nuclear structure physics, heavy-ion collision physics, as well as compact star physics. Nuclear matter is defined as a hypothetical system of nucleons interacting without Coulomb forces, with a fixed ratio of protons and neutrons, and can be supposed as an idealization of matter inside a large nucleus. The aim of nuclear matter theory is to match known experimental bulk properties, such as binding energy, equilibrium density, symmetry energy and incompressibility, starting from fundamental two-body interactions (Pandharipande & Wiringa 1979).

A good many-body theory for nuclear matter can be useful for studying the details of nucleon-nucleon interactions. The observed phase shifts from scattering experiments, plus the properties of the only bound two-nucleon system, the deuteron, are not enough to obtain a unique nucleon–nucleon potential. Nuclear matter studies can help us better understand exactly how the properties of the matter are affected by different elements of a potential, and what sort of features are required to produce the observed saturation. Nuclear matter studies may also indicate whether a potential model for nuclear forces is workable or not (Pandharipande & Wiringa 1979).

The starting point for a microscopic theory of finite nuclei is to solve the infinite matter problem. A solution to the infinite matter problem would also be the first step in obtaining the equation of state for dense matter, which is necessary in the study of neutron stars. At the end, it is simply a very interesting many-body problem in its own right. Methods developed for it should be helpful in other dense quantum fluids such as liquid helium (Pandharipande & Wiringa 1979).

The starting point for any nuclear matter calculation is a two-body potential that models the nucleon-nucleon interaction (Pandharipande & Wiringa 1979). The first nuclear matter calculations were done by Euler (1937). Very little was known about the interaction of nucleons at that time (Pandharipande & Wiringa 1979). At the same time the Yukawa potential was formulated as

$$V = \gamma \frac{\mathrm{e}^{-\mu r}}{r}\,, \tag{1}$$

where γ is a constant, μ is defined as $\frac{\hbar}{M_\pi c} = \frac{1}{\mu}$ (c is the speed of light and M_π is the mass of the π meson) and r is the relative distance between the two nucleons (Cohen 1971; Wong 2007). Several years later, Gammel et al. (1957) introduced a potential of the form

$$V = V_{\mathrm{C}}(r) + V_{\mathrm{T}}(r) S_{12}\,. \tag{2}$$

In Equation (2), $V_{\mathrm{C}}(r)$ is the central potential, $V_{\mathrm{T}}(r)$ is the tensor potential and

$$S_{12} = 3(\sigma_1 \cdot \hat{r})(\sigma_2 \cdot \hat{r}) - \sigma_1 \cdot \sigma_2$$

is the usual tensor operator. Then the potential was allowed to depend at most linearly on the relative momentum $\boldsymbol{p}$, and a spin-orbit term was added to it,

$$V = V_{\mathrm{C}}(r) + V_{\mathrm{T}}(r) S_{12} + V_{ls}(r) \boldsymbol{L} \cdot \boldsymbol{S}\,, \tag{3}$$

where $\boldsymbol{L}$ is the relative angular momentum and $\boldsymbol{S}$ is the total spin of the nucleon pair. This was the form originally proposed by Eisenbud & Wigner (1941).

In 1962 the two most widely used potentials were introduced. Both abandoned the Wigner form. The Hamada & Johnston (1962) model had the form,

$$V = V_{\mathrm{C}}(r) + V_{\mathrm{T}}(r) S_{12} + V_{LS}(r) \boldsymbol{L} \cdot \boldsymbol{S} + V_{LL}(r) L_{12}\,, \tag{4}$$

where

$$L_{12} = [\delta_{LJ} + (\sigma_1 \cdot \sigma_2)] L^2 - (\boldsymbol{L} \cdot \boldsymbol{S})^2$$

and the Yale potential was defined as (Lassila et al. 1962),

$$V = V_{\mathrm{C}}(r) + V_{\mathrm{T}}(r) S_{12} + V_{LS}(r) \boldsymbol{L} \cdot \boldsymbol{S} + V_q(r)[(\boldsymbol{L} \cdot \boldsymbol{S})^2 + \boldsymbol{L} \cdot \boldsymbol{S} - L^2]\,. \tag{5}$$

In 1968 another potential was introduced by Reid (1968). This potential has a central term, $V_{\mathrm{C}}(r)$, for uncoupled states (singlet and triplet with $\boldsymbol{L} = \boldsymbol{J}$) and for coupled states (triplet with $\boldsymbol{L} = \boldsymbol{J} \pm 1$) has the form of Equation (3). In 1974, Bethe & Johnson (1974) (BJ) introduced a potential that had the general form of the Reid potential. The BJ potential has a very hard core in the $(S, T) = (0, 0), (1, 1)$ channels.

In general the above potentials are limited to a few operators and do not fit the data for all the scattering channels very well. In many-body calculations of nuclei and nuclear matter, it is acceptable to represent the two nucleon interaction as an operator (Lagaris & Pandharipande 1981)

$$V_{ij} = \sum_p V^p(r_{ij}) O_{ij}^p\,, \tag{6}$$

where $V^p(r_{ij})$ are functions of the interparticle distance r_{ij}, and O_{ij}^p are suitably chosen operators. The nucleon-nucleon (NN) interaction scattering data uniquely show the occurrence of terms belonging to the eight operators (Lagaris & Pandharipande 1981)

$$O_{ij}^{p=1-8} = 1, \sigma_i \cdot \sigma_j, \tau_i \cdot \tau_j, (\sigma_i \cdot \sigma_j)(\tau_i \cdot \tau_j), S_{ij}, S_{ij}(\tau_i \cdot \tau_j), (\boldsymbol{L} \cdot \boldsymbol{S})_{ij}, (\boldsymbol{L} \cdot \boldsymbol{S})_{ij}(\tau_i \cdot \tau_j) \tag{7}$$

in the V_{ij}. Many nuclear matter calculations have been done with V_8 potential models (Lagaris & Pandharipande 1981). This potential has two different models. One of them is Reid-V_8 (Pandharipande & Wiringa 1979) and the other is the BJ-II V_8 (Pandharipande & Wiringa 1979) model. There is also a V_6 model. The $V_{i=7,8}$ terms are neglected in the V_6 model. The HJ V_6 model is obtained by neglecting the $\boldsymbol{L}\cdot\boldsymbol{S}$ and quadratic spin-orbit terms in the Hamada and Johnston potential (Pandharipande & Wiringa 1979), while the GT-5200 potential (Pandharipande & Wiringa 1979) is itself a V_6 form.

Another NN interaction model is V_{12}. In this model, in addition to the eight operators of Equation (7), there are four momentum-dependent terms

$$O_{ij}^{p=9-12} = L^2, L^2(\sigma_i\cdot\sigma_j), L^2(\tau_i\cdot\tau_j), L^2(\sigma_i\cdot\sigma_j)(\tau_i\cdot\tau_j)\,. \tag{8}$$

The V_{12} potential, like the V_6 model, has two different forms, which are Reid-V_{12} and BJ-II V_{12} (Lagaris & Pandharipande 1981).

In 1981 a phenomenological two-nucleon interaction potential was introduced by Lagaris & Pandharipande (1981). This potential was obtained by fitting the nucleon–nucleon phase shifts up to 425 MeV in S, P, D and F waves, and the deuteron properties. It has two additional terms other than the operators in Eqs. (3) and (4) and is called the V_{14} or $Urbana\ V_{14}$ (UV_{14}) potential.

$$O_{ij}^{p=13,14} = (L\cdot S)^2, (L\cdot S)^2(\tau_i\cdot\tau_j)\,. \tag{9}$$

In the UV_{14} model, the two nucleon interaction is written as

$$V_{ij} = \sum_{p=1,14}\Big(V_\pi^p(r_{ij}) + V_I^p(r_{ij}) + V_S^p(r_{ij})\Big)O_{ij}^p\,, \tag{10}$$

where $V_\pi^p(r_{ij})$ is the well known one-pion-exchange interaction, $V_I^p(r_{ij})$ is an intermediate-range interaction and $V_S^p(r_{ij})$ is a purely phenomenological short-range interaction.

There is also another form of the V_{14} potential which was proposed by Wiringa et al. (1984). It is called the Argonne V_{14} (AV_{14}) potential, and it has the general form of the UV_{14} potential. The difference between the AV_{14} and UV_{14} models is in how the functions $V_\pi^p(r_{ij})$, $V_I^p(r_{ij})$ and $V_S^p(r_{ij})$ are defined.

Traditionally, NN potentials are formed by fitting np data for the $T=0$ states and either np or pp data for the $T=1$ states. Unfortunately, potential models which have been fitted only to the np data often do not give a good description of the pp data (Stoks & de Swart 1993), even after applying the essential correlations for the Coulomb interaction. By the same token, the potentials fit to the pp data in the $T=1$ states simply give a mediocre description of the np data. This problem is largely due to charge-independence breaking in the strong interaction. In the present work we use an updated version of the Argonne potential, the AV_{18} model (Wiringa et al. 1995), which fits both the pp and np data as well as the low-energy nn scattering parameters and deuteron properties. This potential is written in an operator format that depends on the values of S, T and T_Z of the NN pair. The AV_{18} potential includes a charge-independent part that has 14 operator components (as in the AV_{14} model) and a charge-independent breaking part that has three charge-dependent operators and one charge-asymmetric one. The four additional operators that break charge-independence are given by

$$O_{ij}^{p=15-18} = T_{ij}, (\sigma_i\cdot\sigma_j)T_{ij}, S_{ij}T_{ij}, (\tau_{zi}+\tau_{zj})\,, \tag{11}$$

where

$$T_{ij} = 3\tau_{zi}\tau_{zj} - \tau_i.\tau_j$$

is the tensor operator. In between the operators of Equation (11), the first three represent charge-dependence, while the last one represents charge-asymmetry.

In this paper, we use the lowest-order constrained variational (LOCV) method to calculate the correlation function of the nuclear matter. Primarily, the LOCV technique was used to study the bulk properties of quantal fluids (Owen et al. 1977; Modarres & Irvine 1979a). The method was later extended to calculate the symmetry coefficient for the semi-empirical mass formula (Howes et al. 1978a, 1979; Modarres & Irvine 1979a,b), the properties of beta-stable matter (Modarres & Irvine 1979a,b; Howes et al. 1978b), the surface energies of quantal fluids (Howes et al. 1978b) and the binding energies of finite nuclei (Bishop et al. 1978; Modarres 1984). The LOCV method was further extended for finite temperature calculations and was very successfully applied to neutron, nuclear and asymmetrical nuclear matter (Modarres 1993, 1995, 1997) in order to calculate the different thermodynamic properties of these systems. Recently, LOCV calculations have been done for symmetric nuclear matter with phenomenological two-nucleon interaction operators (Bordbar & Modarres 1997) and asymmetrical nuclear matter with the AV_{18} potential (Bordbar & Modarres 1998). The incompressibility of hot asymmetrical nuclear matter has also been investigated within an LOCV approach (Modarres & Bordbar 1998). Very recently, some nucleonic systems such as the spin polarized neutron matter (Bordbar & Bigdeli 2007a), symmetric nuclear matter (Bordbar & Bigdeli 2007b), asymmetrical nuclear matter (Bordbar & Bigdeli 2008a) and neutron star matter (Bordbar & Bigdeli 2008a) at zero temperature have been studied using the LOCV method with a realistic strong interaction in the absence of a magnetic field. The thermodynamic properties of the spin polarized neutron matter (Bordbar & Bigdeli 2008b), symmetric nuclear matter (Bigdeli et al. 2009) and asymmetrical nuclear matter (Bigdeli et al. 2010) have also been studied at finite temperature in the absence of a magnetic field. These calculations have been extended in the presence of a magnetic field for the spin polarized neutron matter at zero temperature (Bordbar et al. 2011). The LOCV method is a fully self-consistent formalism and does not bring any free parameters into the calculation. It considers the normalization constraint to keep the higher order terms as small as possible. The functional minimization procedure represents an enormous computational simplification over unconstrained methods (i.e. to parameterize the short-range behavior of correlation functions) that attempt to go beyond the lowest order (Bordbar & Modarres 1998).

In the present work, we intend to calculate the structure function of asymmetrical nuclear matter using the LOCV method, employing the UV_{14}, AV_{14} and AV_{18} potentials. The plan of this article is as follows. The LOCV method is described in Section 2. Section 3 is devoted to a summary of the pair distribution function and the structure function. Our results and discussion are presented in Section 4, and finally, the summary and conclusions are presented in Section 5.

2 LOCV FORMALISM FOR ASYMMETRICAL NUCLEAR MATTER

We consider a trial many-body wave function of the form

$$\Psi = F\Phi\,, \tag{12}$$

where Φ is a slater determinant of the plane waves of A independent nucleons, F is an A-body correlation operator which will be replaced by a Jastrow form, i.e.

$$F = \mathcal{S}\prod_{i>j} f(ij)\,, \tag{13}$$

and $\mathcal{S}$ is a symmetrizing operator. The cluster expansion of the energy functional is written as

$$E([f]) = \frac{1}{A}\frac{\langle\Psi|H|\Psi\rangle}{\langle\Psi|\Psi\rangle} = E_1 + E_2 + E_3 + \cdots\,. \tag{14}$$

The one-body term E_1 for asymmetrical nuclear matter that consists of Z protons and N neutrons is

$$E_1 = \sum_{i=1,2}\frac{3}{5}\frac{\hbar^2 k_i^{F^2}}{2m_i}\frac{\rho_i}{\rho}\,. \tag{15}$$

Labels 1 and 2 are used instead of proton and neutron, respectively, and $k_i^F = (3\pi^2\rho_i)^{\frac{1}{3}}$ is the Fermi momentum of particle i ($\rho = \rho_1 + \rho_2$).

The two-body energy E_2 is

$$E_2 = \frac{1}{2A}\sum_{ij}\langle ij|\mathcal{V}(12)|ij - ji\rangle \tag{16}$$

and

$$\mathcal{V}(12) = -\frac{\hbar^2}{2m}\big[f(12),[\nabla_{12}^2, f(12)]\big] + f(12)V(12)f(12)\,. \tag{17}$$

The two-body correlation operator $f(12)$ is defined as follows

$$f(ij) = \sum_{\alpha,p=1}^{3} f_\alpha^{(p)}(ij)O_\alpha^{(p)}(ij)\,. \tag{18}$$

$\alpha = \{J, L, S, T, T_z\}$ and the operators $O_\alpha^p(ij)$ are written as

$$O_\alpha^{p=1-3} = 1, \left(\frac{2}{3} + \frac{1}{6}S_{12}\right), \left(\frac{1}{3} - \frac{1}{6}S_{12}\right)\,, \tag{19}$$

where S_{12} is the tensor operator. We choose $p = 1$ for uncoupled channels and $p = 2, 3$ for coupled channels. The two-body nucleon-nucleon interaction $V(12)$ has the following form

$$V(12) = \sum_{p=1}^{18} V^p(r_{12})O_{12}^p\,, \tag{20}$$

where the 18 operators that are defined as before are denoted by the labels $c, \sigma, \tau, \sigma\tau, t$, $t\tau, ls, ls\tau, l2, l2\sigma, l2\tau, l2\sigma\tau, ls2, ls2\tau, T, \sigma T, tT$ and τz (Wiringa et al. 1984). By using correlation operators in the form of Equation (18) and the two-nucleon potential from Equation (20), we find the following equation for the two-body energy (Bordbar & Modarres 1998)

$$\begin{aligned}
E_2 \;=\; & \frac{2}{\pi^4\rho}\left(\frac{\hbar^2}{2m}\right)\sum_{JLSTT_z}(2J+1)\frac{1}{2}\Big[1-(-1)^{L+S+T}\Big] \\
& \times\left|\left\langle\frac{1}{2}\tau_{z1}\frac{1}{2}\tau_{z2}\middle|TT_z\right\rangle\right|^2\int dr\Bigg\{\Bigg[\Big(f_\alpha^{(1)'}\Big)^2 a_\alpha^{(1)^2}(k_Fr) + \frac{2m}{\hbar}\Big(\Big\{V_c - 3V_\sigma \\
& +(V_\tau - 3V_{\sigma\tau})(4T-3) + (V_{\rm T} - 3V_{\sigma T})\times[T(6T_z^2-4)] + 2V_{\tau z}T_z\Big\}a_\alpha^{(1)^2}(k_Fr) \\
& +\Big[V_{l2} - 3V_{l2\sigma}(V_{l2\tau} - 3V_{l2\sigma\tau})(4T-3)\Big]c_\alpha^{(1)^2}(k_Fr)\Big)\Bigg] + \sum_{i=2,3}\Bigg[\Big(f_\alpha^{(i)'}\Big)^2 a_\alpha^{(i)^2} \\
& +\frac{2m}{\hbar^2}\Big(\Big\{V_c + V_\sigma + (-6i+14)V_t - (i-1)V_{ls} + [V_\tau + V_{\sigma\tau} \\
& +(-6i+14)V_{t\tau} - (i-1)V_{ls\tau}](4T-3) + [V_{\rm T} + V_{\sigma T}(-6i+14)V_{tT}] \\
& \times[T(6T_z^2-4)] + 2V_{\tau z}T_z\Big\}a_\alpha^{(i)^2}(k_Fr) + [V_{l2} + V_{l2\sigma} + (V_{l2\tau} + V_{l2\sigma\tau}) \\
& \times(4T-3)]c_\alpha^{(i)^2}(k_Fr) + \Big[V_{ls2} + V_{ls2\tau}(4T-3)\Big]d_\alpha^{(i)^2}(k_Fr)\Big)f_\alpha^{(i)^2}\Bigg] \\
& +\frac{2m}{\hbar^2}\Bigg\{V_{ls} + 2V_{l2} - 2V_{l2\sigma} - 3V_{ls2} + \Big[(V_{ls\tau} - 2V_{l2\tau} - 2V_{l2\sigma\tau} - 3V_{ls2\tau}) \\
& \times(4T-3)\Big]b_\alpha^2(k_Fr)f_\alpha^{(2)}f_\alpha^{(3)} + \frac{1}{r^2}\Big(f_\alpha^{(2)} - f_\alpha^{(3)}\Big)^2 b_\alpha^2(k_Fr)\Bigg\}\Bigg\},
\end{aligned} \tag{21}$$

where the coefficients such as $a_\alpha^{(1)}(x)$ are defined as

$$\begin{aligned}
{a_\alpha^{(1)}}^2(x) &= x^2 I_{L,T_z}(x),\\
{a_\alpha^{(2)}}^2(x) &= x^2[\beta I_{J-1,T_z}(x)+\gamma I_{J+1,T_z}(x)],\\
{a_\alpha^{(3)}}^2(x) &= x^2[\gamma I_{J-1,T_z}(x)+\beta I_{J+1,T_z}(x)],\\
b_\alpha^2(x) &= x^2[\beta_{23} I_{J-1,T_z}(x)-\beta_{23} I_{J+1,T_z}(x)],\\
{c_\alpha^{(1)}}^2(x) &= x^2\nu_1 I_{L,T_z}(x)\,,\\
{c_\alpha^{(2)}}^2(x) &= x^2[\eta_2 I_{J-1,T_z}(x)+\nu_2 I_{J+1,T_z}(x)],\\
{c_\alpha^{(3)}}^2(x) &= x^2[\eta_3 I_{J-1,T_z}(x)+\nu_3 I_{J+1,T_z}(x)],\\
{d_\alpha^{(2)}}^2(x) &= x^2[\xi_2 I_{J-1,T_z}(x)+\lambda_2 I_{J+1,T_z}(x)]\,,\\
{d_\alpha^{(3)}}^2(x) &= x^2[\xi_3 I_{J-1,T_z}(x)+\lambda_3 I_{J+1,T_z}(x)]\,,
\end{aligned} \tag{22}$$

with

$$\begin{aligned}
\beta_1 &= 1, \qquad \beta=\frac{J+1}{2J+1}\,, \qquad \gamma=\frac{J}{2J+1}\,, \qquad \beta_{23}=\frac{2J(J+1)}{2J+1}\,,\\
\nu_1 &= L(L+1)\,, \qquad \nu_2=\frac{J^2(J+1)}{2J+1}\,, \qquad \nu_3=\frac{J^3+2J^2+3J+2}{2J+1}\,,\\
\eta_2 &= \frac{J(J^2+2J+1)}{2J+1}\,, \qquad \eta_3=\frac{J(J^2+J+2)}{2J+1}\,,\\
\xi_3 &= \frac{J^3+2J^2+2J+1}{2J+1}\,, \qquad \xi_3=\frac{J(J^2+J+4)}{2J+1}\,,\\
\lambda_2 &= \frac{J(J^2+J+1)}{2J+1}\,, \qquad \lambda_3=\frac{J^3+2J^2+5J+4}{2J+1}
\end{aligned} \tag{23}$$

and

$$I_{J,T_Z}(x)=\int dq P_{T_Z}(q) J_J^2(xq)\,. \tag{24}$$

$P_{T_Z}(q)$ is written as [τ_{1Z} or $\tau_{2Z}=-\frac{1}{2}$ (neutron) and $+\frac{1}{2}$ (proton)],

$$P_{T_Z}=\frac{2}{3}\pi\left[k_{\tau Z1}^{F^3}+k_{\tau Z2}^{F^3}-\frac{3}{2}\Big(k_{\tau Z1}^{F^2}+k_{\tau Z2}^{F^2}\Big)q-\frac{3}{16}\Big(k_{\tau Z1}^{F^2}-k_{\tau Z2}^{F^2}\Big)^2+q^3\right], \tag{25}$$

for $\frac{1}{2}\left|k_{\tau_{Z1}}^F-k_{\tau_{Z2}}^F\right|<q<\frac{1}{2}\left|k_{\tau_{Z1}}^F+k_{\tau_{Z2}}^F\right|$,

$$P_{T_Z}(q)=\frac{4}{3}\pi\min\left(k_{\tau Z1}^{F^3},k_{\tau Z2}^{F^3}\right),$$

for $q<\frac{1}{2}\left|k_{\tau Z1}^F-k_{\tau Z2}^F\right|$ and

$$P_{T_Z}(q)=0,$$

for $q>\frac{1}{2}\left|k_{\tau Z1}^F+k_{\tau Z2}^F\right|$. The $J_J(x)$ are the familiar Bessel functions.

Now we can minimize the two-body energy, Equation (21), with respect to the variations in the functions f_α^i but subject to the normalization constraint (Owen et al. 1977; Modarres & Irvine 1979a,b; Bordbar & Modarres 1998)

$$\frac{1}{A}\sum_{ij}\left\langle ij\left|h_{T_Z}^2(12)-f^2(12)\right|ij\right\rangle_a=0\,, \tag{26}$$

where in the case of asymmetrical nuclear matter the function $h_{T_Z}(x)$ is defined as

$$h_{T_z}(r) = \left[1 - \frac{9}{2}\left(\frac{J_1(k_i^F r)}{k_i^F r}\right)^2\right]^{-\frac{1}{2}}, \qquad T_z = \pm 1\,, \tag{27}$$
$$h_{T_z}(r) = 1\,, \qquad T_z = 0\,.$$

In terms of channel correlation functions we can write Equation (26) as follows

$$\frac{4}{\pi^4\rho}\sum_{\alpha,i}(2J+1)\frac{1}{2}\Big[1-(-1)^{L+S+T}\Big]\left|\left\langle\frac{1}{2}\tau_{z1}\frac{1}{2}\tau_{z2}\right|TT_z\right\rangle\right|^2 \times\int_0^\infty dr\Big[h^2_{T_z}(k_Fr)-f_\alpha^{(i)^2}(r)\Big]a_\alpha^{(i)^2}(k_Fr)=0\,. \tag{28}$$

As we will see later, the above constraint introduces a Lagrange multiplier λ through which all of the correlation functions are coupled. From the minimization of the two-body cluster energy we get a set of coupled and uncoupled Euler-Lagrange differential equations. The Euler-Lagrange equations for uncoupled states are

$$\begin{aligned} g_\alpha^{(1)''} &- \left\{\frac{a_\alpha^{(1)''}}{a_\alpha^{(1)}}+\frac{m}{\hbar^2}\Big[V_c-3V_\sigma+(V_\tau-3V_{\sigma\tau})(4T-3)\right. \\ &+ (V_{\rm T}-3V_{\sigma T})[T(6T_z^2-4)]+2V_{\tau z}T_z+\lambda\Big]+\frac{m}{\hbar^2}\Big[V_{l2}-3V_{l2\sigma} \\ &+ \left.(V_{l2\tau}-3V_{l2\sigma\tau})(4T-3)\Big]\frac{c_\alpha^{(1)^2}}{a_\alpha^{(1)^2}}\right\}g_\alpha^{(1)}=0, \end{aligned} \tag{29}$$

while the coupled equations are written as

$$\begin{aligned} g_\alpha^{(2)''} &- \left\{\frac{a_\alpha^{(2)''}}{a_\alpha^{(2)}}+\frac{m}{\hbar^2}\Big[V_c+V_\sigma+2V_t-V_{ls}+(V_\tau+V_{\sigma\tau}+2V_{t\tau}\right. \\ &- V_{ls\tau})(4T-3)+(V_{\rm T}+V_{\sigma T}+2V_{tT})[T(6T_z^2-4)]+2V_{\tau z}T_z+\lambda\Big] \\ &+ \frac{m}{\hbar^2}\Big[V_{l2}+V_{l2\sigma}+(V_{l2\tau}+V_{l2\sigma\tau})(4T-3)\Big]\frac{c_\alpha^{(2)^2}}{a_\alpha^{(2)^2}}+\frac{m}{\hbar^2}\Big[V_{ls2}+V_{ls2\tau} \\ &\times (4T-3)\Big]\frac{d_\alpha^{(2)^2}}{a_\alpha^{(2)^2}}+\frac{b_\alpha^2}{r^2a_\alpha^{(2)^2}}\Big\}g_\alpha^{(2)}+\left\{\frac{1}{r^2}-\frac{m}{2\hbar^2}\Big[V_{ls}-2V_{l2}-2V_{l2\sigma}\right. \\ &- \left.3V_{ls2}+(V_{ls\tau}-2V_{l2\tau}-2V_{l2\sigma\tau}-3V_{ls2\tau})(4T-3)\Big]\right\} \\ &\times \frac{b_\alpha^2}{a_\alpha^{(2)}a_\alpha^{(3)}}g_\alpha^{(3)}=0\,, \end{aligned} \tag{30}$$

$$
\begin{aligned}
g_\alpha^{(3)''} &- \left\{\frac{a_\alpha^{(3)''}}{a_\alpha^{(3)}} + \frac{m}{\hbar^2}\Big[V_c + V_\sigma - 4V_t - 2V_{ls} + (V_\tau + V_{\sigma\tau} - 4V_{t\tau}\right.\\
&- \left. 2V_{ls\tau})(4T-3) + (V_{\rm T} + V_{\sigma T} - 4V_{tT})[T(6T_z^2-4)] + 2V_{\tau z}T_z + \lambda\Big]\right.\\
&+ \frac{m}{\hbar^2}\Big[V_{l2} + V_{l2\sigma} + (V_{l2\tau} + V_{l2\sigma\tau})(4T-3)\Big]\frac{c_\alpha^{(3)^2}}{a_\alpha^{(3)^2}} + \frac{m}{\hbar^2}\Big[V_{ls2} + V_{ls2\tau}\\
&\times (4T-3)\Big]\frac{d_\alpha^{(3)^2}}{a_\alpha^{(3)^2}} + \frac{b_\alpha^2}{r^2 a_\alpha^{(2)^2}}\Big\}g_\alpha^{(3)} + \left\{\frac{1}{r^2} - \frac{m}{2\hbar^2}\Big[V_{ls} - 2V_{l2} - 2V_{l2\sigma}\right.\\
&- \left. 3V_{ls2} + (V_{ls\tau} - 2V_{l2\tau} - 2V_{l2\sigma\tau} - 3V_{ls2\tau})(4T-3)\Big]\right\}\\
&\times \frac{b_\alpha^2}{a_\alpha^{(2)}a_\alpha^{(3)}}g_\alpha^{(2)} = 0\,, \qquad (31)
\end{aligned}
$$

where

$$g_\alpha^{(i)}(k_F r) = f_\alpha^{(i)}(r)a_\alpha^{(i)}(k_F r)\,. \qquad (32)$$

The primes in the above equation mean differentiation with respect to r. As we pointed out before, the Lagrange multiplier λ is associated with the normalization constraint, Eq. (28). The constraint is incorporated by solving the Euler-Lagrange equations only out to certain distances, until the logarithmic derivative of the correlation functions matches those of $h_{T_Z}(r)$ and then we set the correlation functions equal to $h_{T_Z}(r)$ (beyond these state-dependent healing distances) (Bordbar & Modarres 1998). Finally, by numerically solving the above differential equations (Eqs. (29), (30) and (31)), we obtain the correlation functions.

3 STRUCTURE FUNCTION

There are two types of structure functions: dynamic $S(\boldsymbol{k}, w)$ and static $S(\boldsymbol{k})$. They measure the response of the system to density fluctuations (Feenberg 1969).

The static structure function of a system consisting of A particles is defined as (Feenberg 1969)

$$S(\boldsymbol{k}) = 1 + \frac{1}{A}\int d^3r_1 d^3r_2 \mathrm{e}^{i\boldsymbol{k}\cdot\boldsymbol{r}_{12}}\rho_1(\boldsymbol{r}_1)\rho_1(\boldsymbol{r}_2)[g(\boldsymbol{r}_1,\boldsymbol{r}_2)-1]\,, \qquad (33)$$

where $\rho_1(\boldsymbol{r})$ is the one-particle density and $g(\boldsymbol{r}_1,\boldsymbol{r}_2)$ is the pair distribution function. In infinite systems, $\rho_1(\boldsymbol{r})$ is constant ($=\rho$) and g is a function of the interparticle distance $r_{12} = |\boldsymbol{r}_1 - \boldsymbol{r}_2|$, therefore Equation (33) takes the following form,

$$S(\boldsymbol{k}) = 1 + \rho\int \mathrm{e}^{i\boldsymbol{k}\cdot\boldsymbol{r}_{12}}[g(r_{12})-1]d^3r_{12}\,. \qquad (34)$$

For calculating the pair distribution function, we use the lowest order term in the cluster expansion of $g(r_{12})$ as follows (Clark 1979),

$$g(r_{12}) = f^2(r_{12})g_F(r_{12})\,, \qquad (35)$$

where $f(r_{12})$ is the two-body correlation function and $g_F(r_{12})$ is the two-body radial distribution function of the noninteracting Fermi-gas,

$$g_F(r_{12}) = 1 - \frac{1}{\nu}l^2(k_F r_{12})\,. \qquad (36)$$

In the above equation, ν is the degeneracy factor, and $l(x) = 3x^{-3}(\sin x - x\cos x)$ is the statistical correlation function or the Slater factor.

4 RESULTS AND DISCUSSION

4.1 Correlation Function

In Figure 1, we plotted our results for the correlation function of symmetrical nuclear matter versus internucleon distance ($r_{12} = r$) employing UV_{14}, AV_{14} and AV_{18} potentials at density $\rho = 0.16\ \mathrm{fm}^{-3}$. Here the correlation functions are calculated from the average over all states. We can see that the correlation function is zero at the internucleon distance $r < 0.06\ \mathrm{fm}$ for the three potentials. This distance represents the famous hard core of the nucleon-nucleon potential. When the internucleon distance increases, the correlation also increases until it approaches unity, approximately at $r > 3.8\ \mathrm{fm}$. This means that at r greater than the above value, the nucleons are out of the range of the nuclear force (correlation length). The correlation value for the AV_{18} potential has a maximum greater than unity and then approaches unity. However, for the UV_{14} and AV_{14} potentials, there is no such maximum.

In Figure 2, we plotted the correlation function of asymmetrical nuclear matter employing the AV_{18} potential for different values of proton to neutron ratio (pnrat =0.2, 0.6, 1.0) at different isospin channels (nn, np, pp). From this figure, it can be seen that for all values of pnrat, the correlation functions of the nn and pp channels have maximums greater than unity, whereas at the np channel there is no such maximum. This means that at the pp and nn channels, the nucleon-nucleon potential is more attractive than at the np channel.

We can see that at the nn and pp channels, the maximum values of the correlation function decrease with increasing pnrat. We also found that at the pp and np channels, the correlation length decreases as pnrat increases, while at the nn channel, with increasing pnrat, the correlation length increases. In addition, for each pnrat, the value of the correlation length at the pp channel is greater than that of the np channel, and the correlation length at the nn channel has a greater value than the pp channel. These have been clarified in Table 1, in which the values of the correlation length for different values of pnrat at different isospin channels have been presented.

Table 1 Correlation Length of Asymmetrical Nuclear Matter

pnrat	Correlation Length (fm)		
	nn	np	pp
0.2	2.95	2.09	2.18
0.6	3.36	1.97	2.11
1.0	3.39	1.94	2.06

4.2 Pair Distribution Function

We know that the pair distribution function, $g(r)$, represents the probability of finding two particles at the relative distance of r. In Figure 3, we plotted our results for the pair distribution function of symmetrical nuclear matter versus internucleon distance with UV_{14}, AV_{14} and AV_{18} potentials at density $\rho = 0.16\ \mathrm{fm}^{-3}$. Our results are in good agreement with those of other calculations employing the Reid potential (Modarres 1987).

Figure 3 shows that for r in the range 1.1 to $3.4\ \mathrm{fm}$, the pair distribution function corresponding to the AV_{18} potential is greater than those of the UV_{14} and AV_{14} potentials. This is due to the behavior of two-body correlation as mentioned in the above discussions. In the Fermi gas model, due to the absence of interaction between nucleons, the pair distribution function is not zero even in the small internucleon distances shown in Figure 3. However, in the real system, in which there is interaction between nucleons, the value of $g(r)$ at $r < 0.06\ \mathrm{fm}$ is zero for the three potentials. This is the same as for the case of the correlation function, and this distance represents the hard core of the

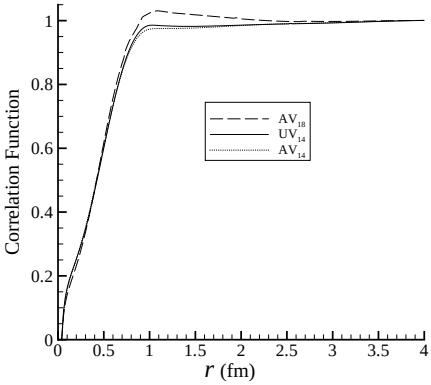

Fig. 1 Correlation function of symmetrical nuclear matter employing UV_{14}, AV_{14} and AV_{18} potentials. The correlation functions have been calculated from the average over all states.

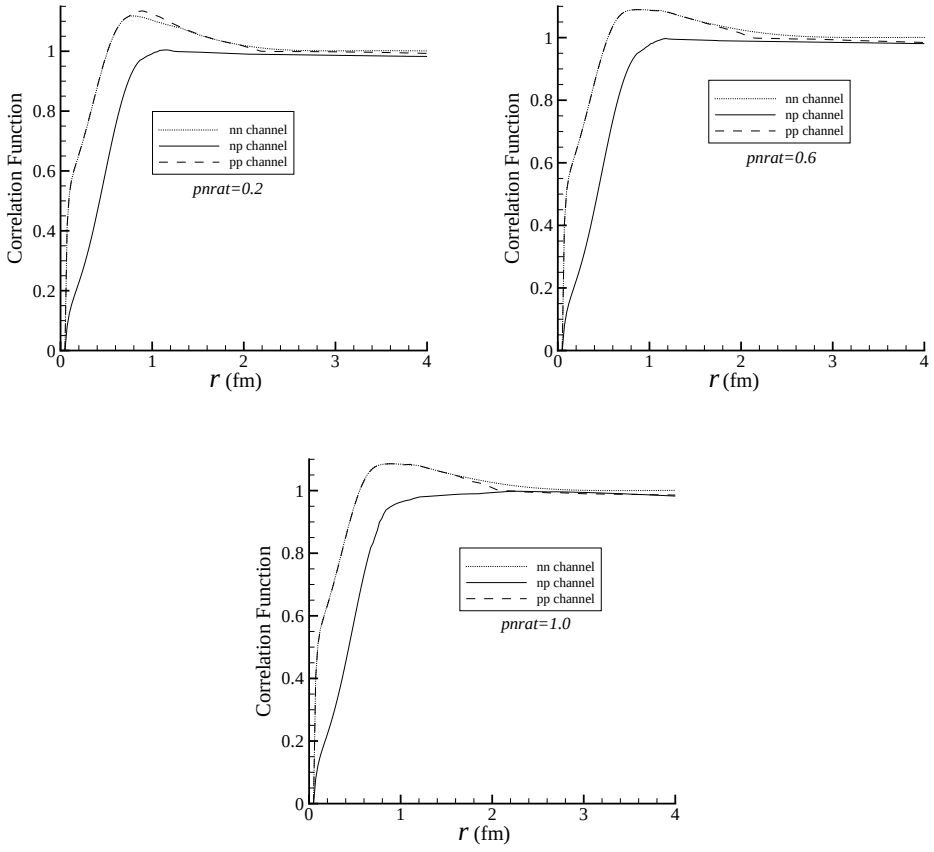

Fig. 2 Correlation function of asymmetrical nuclear matter employing the AV_{18} potential for $\rho = 0.16\ \mathrm{fm}^{-3}$ and different values of pnrat at different isospin channels (nn, pp and np).

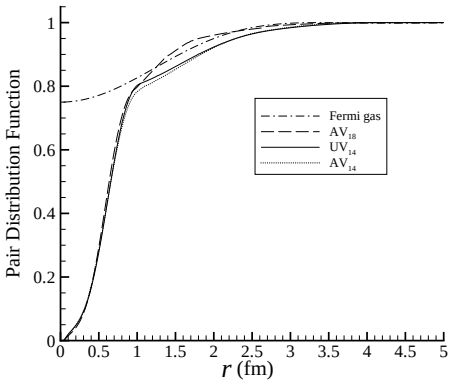

Fig. 3 Pair distribution function for symmetrical nuclear matter calculated with UV_{14}, AV_{14} and AV_{18} potentials at density $\rho = 0.16$ fm^{-3}. The pair distribution function corresponding to the Fermi gas is also provided for comparison.

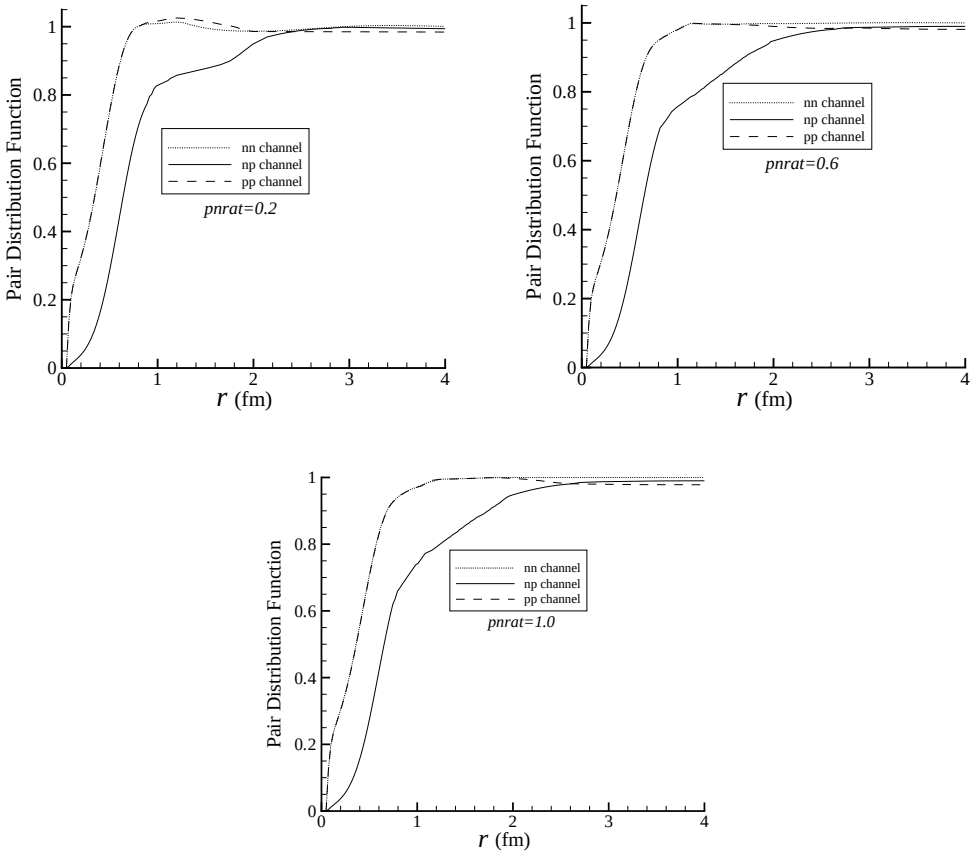

Fig. 4 Same as Fig. 2, but for the pair distribution function of asymmetrical nuclear matter.

nuclear potential. From Figure 3, it can be seen that the value of $g(r)$ increases as the internucleon distance increases and finally approaches unity at approximately $r > 4$ fm.

In Figure 4, we plotted the pair distribution function of asymmetrical nuclear matter employing the AV_{18} potential at different values of proton to neutron ratio (pnrat) for $\rho = 0.16$ fm^{-3} and different isospin channels (nn, np, pp). We can see that at all channels, by increasing pnrat, the pair distribution function decreases, corresponding to a decrease in the correlation. Besides, from Figure 4 it can be seen that for each pnrat, the pair distribution functions of the nn and pp channels have identical behaviors, while at the np channel, $g(r)$ behaves differently compared to the other two channels. These are corresponding to the behavior of the correlation function at these channels.

4.3 Structure Function

In Figure 5, we plotted our results for the structure function of symmetrical nuclear matter versus relative momentum (k) with UV_{14}, AV_{14} and AV_{18} potentials at density $\rho = 0.16$ fm^{-3}. There is an overall agreement between our results and those of others calculated with the Reid potential (Modarres 1987). From Figure 5, it is seen that the nucleon–nucleon interaction leads to a reduction of the structure function of nuclear matter with respect to that of the non-interacting Fermi gas system.

In Figure 6, we plotted the structure function of asymmetrical nuclear matter with the AV_{18} potential at different isospin channels (nn, np, pp) for different values of proton to neutron ratio (pnrat) and $\rho = 0.16$ fm^{-3}. It is seen that, in a similar way to the pair distribution function, the structure function of the nn channel is like that of the pp channel, especially at higher values of k. We found that this similarity becomes clearer as pnrat increases. However, there is a substantial difference between the structure functions of the np channel and the pp and nn channels.

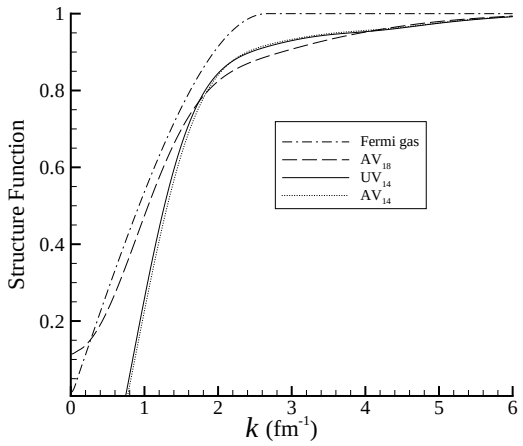

Fig. 5 Structure function of symmetrical nuclear matter with UV_{14}, AV_{14} and AV_{18} potentials at density $\rho = 0.16$ fm^{-3}.

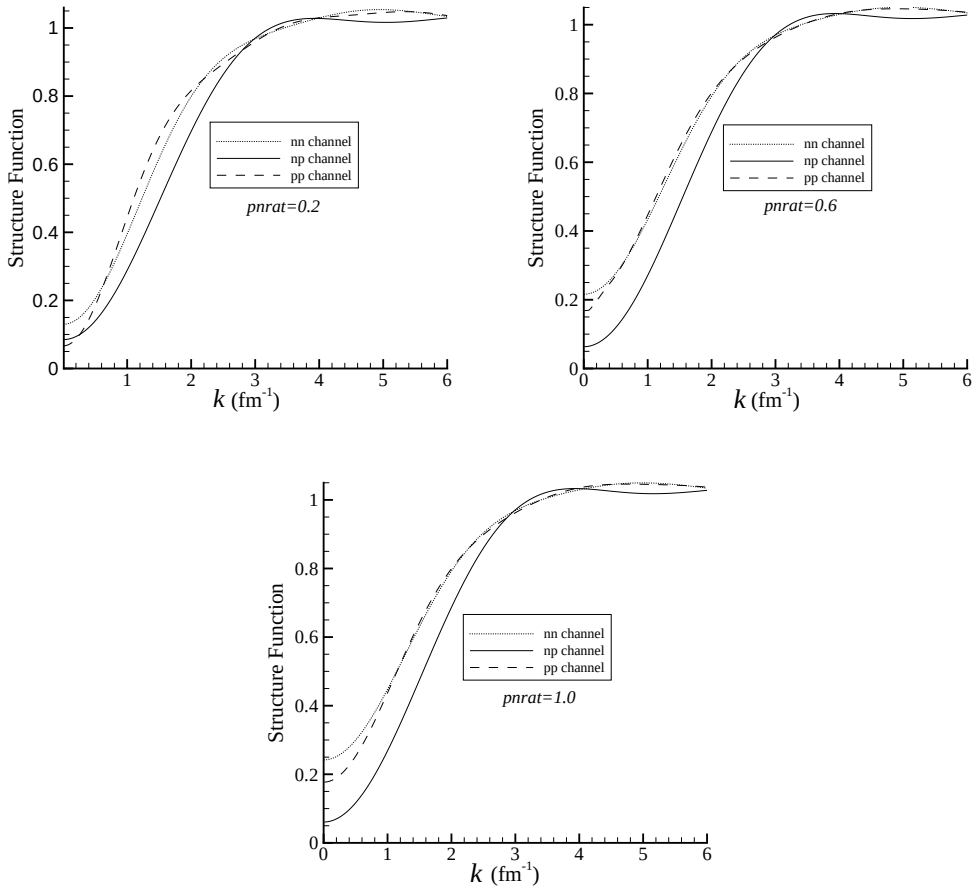

Fig. 6 Same as Fig. 2, but for the structure function of asymmetrical nuclear matter.

5 SUMMARY AND CONCLUSIONS

Using the LOCV method, we computed the correlation function, pair distribution function and the structure function of the symmetrical and asymmetrical nuclear matter. In order to investigate the effect of nucleon-nucleon interaction on the properties of nuclear matter, we also computed the pair distribution function and structure function of noninteracting Fermi gas. Here, we used the AV_{18} potential to represent the nucleon-nucleon interaction for the asymmetrical nuclear matter. These calculations were performed at different isospin channels. In the case of symmetrical nuclear matter, the calculations were done with UV_{14}, AV_{14} and AV_{18} potentials. There is an overall agreement between our results and those of others calculated with the Reid potential. It was seen that the nucleon–nucleon interaction leads to the reduction of the structure function of nuclear matter with respect to that of the non-interacting Fermi gas system. We found that at the np and pp channels, the correlation length decreases as the proton to neutron ratio (pnrat) increases, while at the nn channel, by increasing pnrat, the correlation length increases. However, the behavior of the pair distribution function at the np channel is considerably different from the other two channels. This is due to the difference between the behavior of the correlation functions of these channels. It was indicated that for higher k and pnrat, the structure functions of the nn and pp channels are identical, corresponding

to the similarity between the pair distribution functions of these channels. We have also shown that the structure function at the np channel was different from those of the nn and pp channels.

Acknowledgements This work was supported by the Research Institute for Astronomy and Astrophysics of Maragha. We wish to thank the Shiraz University Research Council.

References

Bethe, H. A., & Johnson, M. B. 1974, Nuclear Physics A, 230, 1
Bigdeli, M., Bordbar, G. H., & Poostforush, A. 2010, Phys. Rev. C, 82, 034309
Bigdeli, M., Bordbar, G. H., & Rezaei, Z. 2009, Phys. Rev. C, 80, 034310
Bishop, R. F., Howes, C., Irvine, J. M., & Modarres, M. 1978, Journal of Physics G Nuclear Physics, 4, 1709
Bordbar, G. H., & Bigdeli, M. 2007a, Phys. Rev. C, 75, 045804
Bordbar, G. H., & Bigdeli, M. 2007b, Phys. Rev. C, 76, 035803
Bordbar, G. H., & Bigdeli, M. 2008a, Phys. Rev. C, 77, 015805
Bordbar, G. H., & Bigdeli, M. 2008b, Phys. Rev. C, 78, 054315
Bordbar, G. H., & Modarres, M. 1997, Journal of Physics G Nuclear Physics, 23, 1631
Bordbar, G. H., & Modarres, M. 1998, Phys. Rev. C, 57, 714
Bordbar, G. H., Rezaei, Z., & Montakhab, A. 2011, Phys. Rev. C, 83, 044310
Clark, J. W. 1979, Progress in Particle and Nuclear Physics, 2, 89
Cohen, B. L. 1971, Concepts of nuclear physics (Tata McGraw-Hill Education)
Eisenbud, L., & Wigner, E. P. 1941, Proceedings of the National Academy of Science, 27, 281
Euler, H. 1937, Zeitschrift fur Physik, 105, 553
Feenberg, E. 1969, Theory of Quantum Fluids (Academic Press)
Gammel, J. L., Christian, R. S., & Thaler, R. M. 1957, Physical Review, 105, 311
Hamada, T., & Johnston, I. D. 1962, Nucl. Phys. A, 34, 382
Howes, C., Bishop, R. F., & Irvine, J. M. 1978a, Journal of Physics G Nuclear Physics, 4, L81
Howes, C., Bishop, R. F., & Irvine, J. M. 1978b, Journal of Physics G Nuclear Physics, 4, L123
Howes, C., Bishop, R. F., & Irvine, J. M. 1979, Journal of Physics G Nuclear Physics, 4, 11
Lagaris, I. E., & Pandharipande, V. R. 1981, Nuclear Physics A, 359, 331
Lassila, K. E., Hull, M. H., Ruppel, H. M., McDonald, F. A., & Breit, G. 1962, Physical Review, 126, 881
Modarres, M. 1984, Journal of Physics G Nuclear Physics, 10, L251
Modarres, M. 1987, Journal of Physics G Nuclear Physics, 13, 755
Modarres, M. 1993, Journal of Physics G Nuclear Physics, 19, 1349
Modarres, M. 1995, Journal of Physics G Nuclear Physics, 21, 351
Modarres, M. 1997, Journal of Physics G Nuclear Physics, 23, 923
Modarres, M., & Bordbar, G. H. 1998, Phys. Rev. C, 58, 2781
Modarres, M., & Irvine, J. M. 1979a, Journal of Physics G Nuclear Physics, 5, 511
Modarres, M., & Irvine, J. M. 1979b, Journal of Physics G Nuclear Physics, 5, L7
Owen, J. C., Bishop, R. F., & Irvine, J. M. 1977, Nuclear Physics A, 277, 45
Pandharipande, V. R., & Wiringa, R. B. 1979, Reviews of Modern Physics, 51, 821
Reid, R. V., Jr. 1968, Annals of Physics, 50, 411
Stoks, V., & de Swart, J. J. 1993, Phys. Rev. C, 47, 761
Wiringa, R. B., Smith, R. A., & Ainsworth, T. L. 1984, Phys. Rev. C, 29, 1207
Wiringa, R. B., Stoks, V. G. J., & Schiavilla, R. 1995, Phys. Rev. C, 51, 38
Wong, S. S. M. 2007, in Introductory Nuclear Physics, Second Edition (Wiley-VCH Verlag GmbH, Weinheim, Germany. doi: 10.1002/9783527617906.ch1)